

# We are IntechOpen, the world's leading publisher of Open Access books Built by scientists, for scientists

4,800

Open access books available

122,000

International authors and editors

135M

Downloads

Our authors are among the

154

Countries delivered to

TOP 1%

most cited scientists

12.2%

Contributors from top 500 universities



WEB OF SCIENCE™

Selection of our books indexed in the Book Citation Index  
in Web of Science™ Core Collection (BKCI)

Interested in publishing with us?  
Contact [book.department@intechopen.com](mailto:book.department@intechopen.com)

Numbers displayed above are based on latest data collected.  
For more information visit [www.intechopen.com](http://www.intechopen.com)



# Sediment Gravity Flows: Study Based on Experimental Simulations

Rafael Manica

*Instituto de Pesquisas Hidráulicas - Universidade Federal do Rio Grande do Sul  
Brazil*

## 1. Introduction

Gravity (or density currents) currents are a general class of flows (also known as stratified flows) in which flow takes place because of relatively small differences in density between two flows (Middleton, 1993). Gravity currents that are driven by gravity acting on dispersed sediment in the flow were called *sediment gravity flows* (Middleton & Hampton, 1973). Sediment gravity flows may occur in both subaerial (e.g. avalanches, pyroclastic flows and so on) and subaqueous ambients (e.g. bottom currents, turbidity currents, debris flow – see Simpson, 1997) and may flow above, below or inside the ambient fluid. The distinction regarding sediment gravity flows and open-channel flows is due to the order of magnitude of the density difference between the fluids. Sediment gravity flow are generally of the same order of magnitude, whilst open-channel flow the difference in density between the flow (e.g. rivers) and the ambient air is much higher than that.

The interest in these types of flows are mainly due to four factors: (i) phenomenon comprehension highlighting the origin, transport and deposition processes; (ii) their great magnitude and unpredictability (potential environmental hazards); (iii) the lack of monitoring these events in nature and; (iv) because of their economic significance, since some deposits generated by such currents are prospective reserves of hydrocarbon.

Despite the great progress addressing theoretical and analytical evaluation of these phenomena, particularly on the origin, transport and deposition of this class of flow, even today, they are not completely comprehended. Generally, the complexity of the phenomenon can be expressed by: (i) interaction between the flow and the bed morphology; (ii) the quantity and the composition of sediment transported and (iii) the complex mixing processes. As a consequence, the origin and the hydrodynamics properties of these flows are less understood than open-channel flows (Baas et al., 2004). Simple definitions, such as volumetric concentrations of sediments, its composition and size distribution of solid particles in the mixture as well as the sediment-support mechanisms are difficult to measure in nature which is also an indicative of such complexity.

Kneller & Buckee (2000) commented that difficulties in understanding the dynamics of suspended sediment are extremely complex by virtue of turbulence. In that case, the phenomenon is: non-linear; non-uniform (variation in space) and unsteady (variation in time). If the flow contains large loads of sediments and/or cohesive sediments in suspension this complexity increases even more. Besides the variation of density with time and space (open boundary conditions), the mechanical properties (rheology) of the suspensions

involved (thixotropy, viscosity and gravitational forces) must be taken into account as well as the sediment-support mechanism and the influence of shear stress on the upper layer (Kuenen, 1950). Because of such uncertainty and complexity, many terms, concepts, models and particular descriptions (over than 30) have being introduced and applied to interpret these classes of flows and deposits along the years (e.g. Gani, 2004; Lowe, 1982; Middleton & Hampton, 1973).

Sediment gravity flows can be divided into five broad categories according to Parsons et al., (2010). Each flow type has a range of concentrations, Reynolds numbers, duration, grain size and rheology behaviour, enclosing a general overview of the flows transformation along time and space (Fischer, 1983). Two types of flows have been regularly studied along the last 60 years: turbidity currents and debris flows. Both represent the contrast of the sediment gravity flows categories (not considering mass flows, like slides and slumps - see also Middleton & Hampton, 1973). Succinctly, the main properties attributed and well accepted in the literature to turbidity currents are: diluted (low-density), Newtonian behaviour, turbulent regime, and Bouma sequence type deposit (Bouma, 1962) usually called turbidites. On the other side, debris flows are characterized by great influence of non-cohesive material, non-Newtonian behaviour, matrix strength, bipartite and chaotic (ungraded) deposits.

The interest of many fields of academy and industry do not only concern the comprehension of those two particular types of flows. In fact, all classes of sedimentary gravity currents are motivating researchers to face the problem from different approaches and methods, for instance: studies based on outcrops analogy (generally by sedimentologists and correlated areas); numerical and analytical modelling (which is improving through time) and, finally experimental simulation which has been a powerful tool of visualization and measurement of flow dynamics properties as well as of generated deposit.

The scope of this chapter is to outline the experimental study on sediment gravity flows in order to characterize and comprehend this phenomenon regarding their rheological behaviour, hydrodynamics and depositional properties. The simulations covered a wide range of concentration and/or different amount of cohesive sediments in the mixture. The properties of the flow and deposit were evaluated, classified and compared to literature background. The chapter is structured in five sections; first, a general description of sediment gravity flows will be presented followed by the experimental approach applied. Then, the rheology tests it will be reported and finally, the careful evaluation of the experimental results in terms of time-space and vertical profiles will be described in order to extrapolate the results to natural sediment gravity flows.

### 1.1 Sediment gravity flow anatomy

In nature, subaqueous sediment gravity flow behaves like a river system, i.e., originating (source zone), flowing (transfer zone) and decelerating up to the point where all suspended sediment settled down (depositional zone). In general, the initiation of sediment gravity flows is strongly related to two processes of sediment remobilization in the natural field: Firstly, by the occurrence of catastrophic events such as earthquakes, sedimentary failures, storms and volcanic eruptions which cause high instabilities and remobilize large amount of sediments instantaneously (Normark & Piper, 1991); Secondly, by continuous river supply in which the river discharge is connected into water body (usually reservoirs, lakes and oceans) generating plumes and/or hyperpycnal flows due the density difference (positive or negative). After the process starts, the mixture of suspended sediment (concentration, size

and composition) is transported ahead by the flow (transfer zone). Concomitantly, dynamical and depositional processes occur along time and space, causing flow transformations, such as: sediment transport, erosion and/or deposition, mixing, entrainment (Elisson & Turner, 1959) and so on (Fig. 1).

The sediment gravity flows which maintain buoyancy flux throughout movement are called *conservative* (i.e. do not interact with their boundary). Otherwise, flows are called *non-conservative sediment gravity flows* (i.e. open boundary interaction such as erosion and deposition).

Generally, gravity currents are divided geometrically into three distinct parts: head, body and, tail.

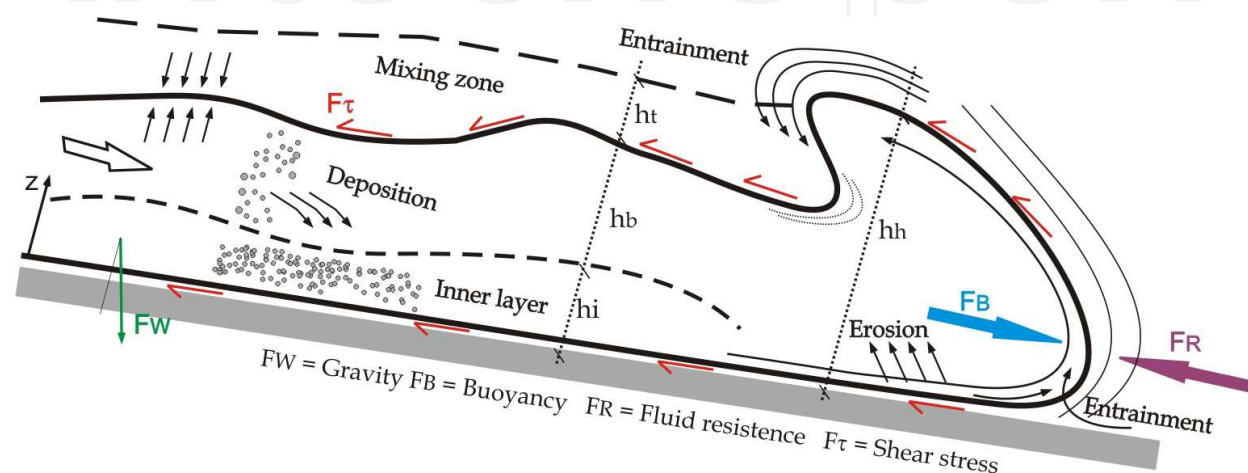


Fig. 1. Schematic of a sediment gravity flow (description of all terms is provided in the list of nomenclature).

The *head* or front of the current is roughly shaped as a semiellipse. In most cases, the head is thicker than the body and tail, because of the resistance imposed by the ambient fluid (fluid resistance) to its advance. The head plays an important role on flow dynamics because is characterized by strong three-dimensionality effects and intense mixing (Simpson, 1997). The most advanced point of the front is called *nose* and it is located slightly above the bottom surface, as a result of the no-slip condition at the bottom as well as the resistance (shear) at upper surface (Britter & Simpson, 1978). In the head, two types of instabilities are the main responsible for mixing with the ambient fluid (*entrainment*). The first type of instability is a complex pattern of *lobes and clefts* caused by second order gravitational instabilities at front surface (Kneller et al., 1999; Simpson, 1972). The second type of instability is a series of billows associate to Kelvin-Helmholtz instabilities (Britter & Simpson, 1978), which takes place just behind the head and produced by viscous shear at the head and body (upper surface). This zone behind head creates a large-scale turbulence mixing and also divides the head from the body (symbolically called: *neck* of the flow).

Generally, the velocity of the *body* is greater than the head velocity by 30% or 40% (Baas et al., 2004; Kneller & Buckee, 2000). One reason for this is the presence of a large billow behind the head which cause a locally diluted zone (entrainment of ambient fluid). Thus, in order to the flow maintain its constant rate of advance, the current increases the velocity of the body to compensate the deficit of density created (Middleton, 1993). The body is divided into two zones: near the bottom zone, where the density is higher; and above this, a suspended/mixing zone, where the mixing with the fluid ambient occurs. The interface

between these layers (bipartite flow) point out a discontinuity in the body (water-column stratification) that is reflected by an abrupt gradient of velocity, concentration and viscosity (Postma et al., 1988).

The third part of sediment gravity flow is characterized by a deceleration zone and final dilution stage of the current, normally called *tail*.

In terms of dynamics properties of the flow, sediment gravity flows differ significantly from open-channel flows (e.g. rivers) regarding their velocity profile. In that case of sediment gravity flow, the main difference is due to the fact that is not possible to ignore the shear effects in the upper surface of the current (see Fig. 2 a, b). Then, the sediment gravity flows velocity profile has null values at the upper and bottom surfaces and values grow towards to the middle (balance of drag forces acting on those surfaces), creating a front point (maximum value) usually at 0.2 to 0.3 times the height of the current. Depending on the concentration and composition of sediments in suspension, both velocity and concentration profiles may present completely different shape (Fig. 2 c) as the inner dynamic of the flow became more complex (e.g. matrix strength, cohesive forces).

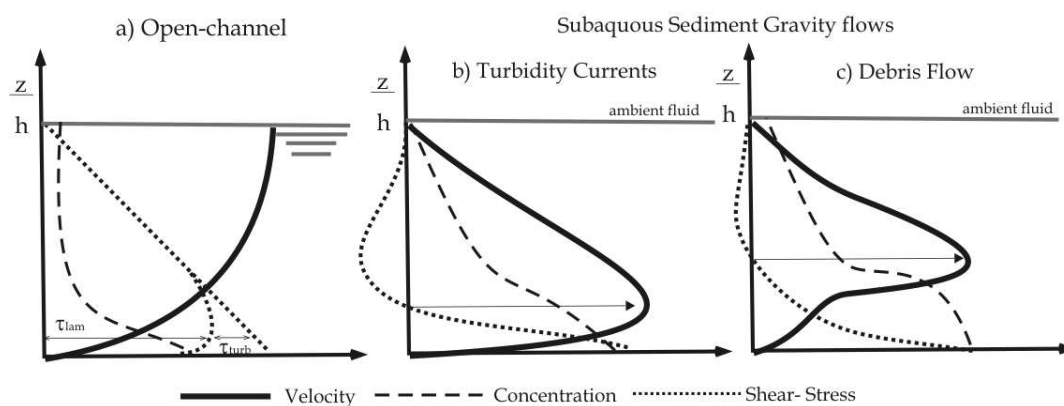


Fig. 2. Vertical profiles of velocity, concentration and shear stress for: a) open-channel flows; b) turbidity current and; c) debris Flow.

The two most known classes of sedimentary gravity flows (described earlier) have differences regarding their internal dynamics. The dynamics of turbidity currents is complex due to the processes of erosion and deposition. Because of this, the three-dimensional representation of this phenomenon through analytical equations is not simple, which leads to simplification (e.g. shallow water flows – Parson et al., 2010; Parker et al., 1986). In the same way, the debris flows are extremely complex too, as the existence of yield strength caused by the high density and the presence of clay implies in shear-like flow and plug-like flows as illustrated in Fig. 3.

Generally, the hydrodynamic of a sediment gravity flow is closely associated to sediment-transport capacity (total amount of sediment transported by the flow) and competence (ability of the flow to carry particular grain size) as well as to the sediment-support mechanism, whose the main role is to keep the sediments in suspension for a long period of time (and distance). For each class of flow may occur different mechanisms of sediment-support, as it depends on grain-size and composition, concentration of sediments and the rheological properties of the mixture.

For turbidity currents, the main sediment-support mechanisms are vertical component of turbulence and buoyancy. However, for flows of high concentration (high-density) several



sediment-support mechanisms may occur simultaneously, such as: *hindered settling*, in which grains deposition is inhibited because the number of particles increases in an certain zone, creating a slower-moving mixture than would normally be expected (effect of population of grains); *dispersive pressure*: in which the grains are held in suspension by their interaction forces (collision) and; *matrix strength*: a mixture of interstitial fluid and fine sediment (cohesive), which has a finite yield strength that supports coarse grains (Lowe, 1979; Middleton & Hampton, 1973).

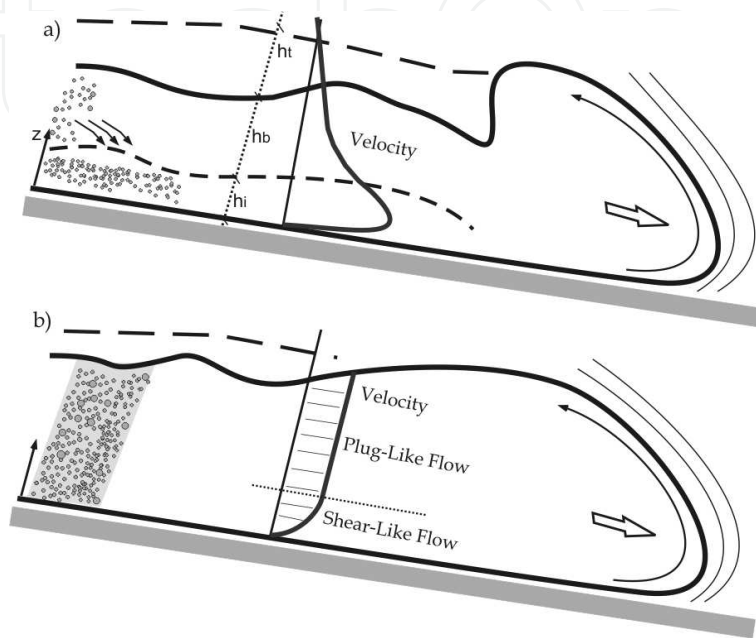


Fig. 3. The difference between the internal dynamics of the turbidity current (a) and debris flow (b).

The effect of high concentration on the dynamics of sediment gravity flows is expressed by changes in the mixture and flow properties such as: density of the fluid; increase of the potential energy and momentum of the flow and; viscosity of the mixture (rheological behaviour). Also, the settling velocity of particles is strongly influenced by the increase in fluid concentration mainly because: the fall of the particles induces an upward movement of water; the buoyancy of the particle increases due to high-density fluid, and by the interaction between particles (effect of population - *hindered settling*). The transport capacity of the flow tends to increase with high sediment concentration; however, these changes also depend on the composition of sediment present in suspension.

In contrast, the presence of cohesive sediment implies a different scenario in which the flocs of cohesive particles will settle down during the flow, creating a clay/mud near-bed layer with high content of water inside. Despite the fact the turbulence can be produced in this clay/mud layer (due to shear flow), there is also a significant increase in viscous forces (non-Newtonian behaviour), which could reduced the flow ability to transport great amounts of sediment downstream.

## 2. Apparatus and experimental simulations

In order to understand the hydrodynamic of natural sediment gravity, an experimental study was performed with different types of sediments, such as: non-cohesive particles

represented by very fine sand and silt sized glass beads, and cohesive particles represented by kaolin clay. Both sediments have density approximately of  $2600 \text{ kg/m}^3$ . In total, 21 experiments (Fig. 4) were carried out with eight values of bulk volumetric concentration (2.5%, 5%, 10%, 15%, 20%, 25%, 30% and 35%). In addition, for each value of concentration were used three different proportions of clay in the mixture from 0% (pure non-cohesive flows) passing to 50% (mixed) and finally, 100% (pure cohesive flows).

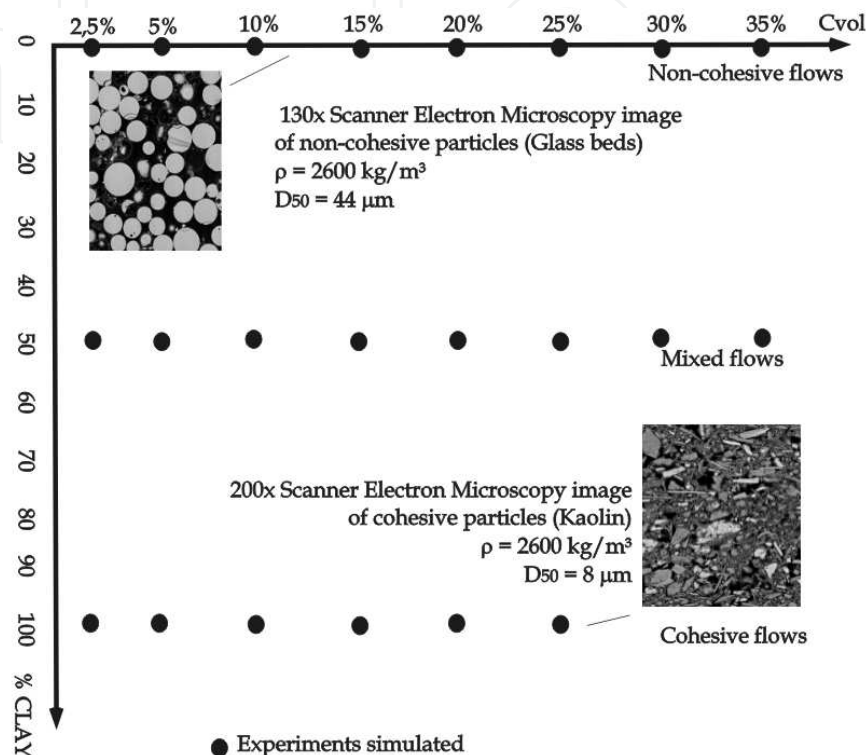


Fig. 4. Initial properties of the mixtures simulated and the particles properties.

The experiments were performed in a 2D Perspex tank (4.50 m long x 0.20 m wide x 0.50 m height). A 120 litres mixture was prepared in a mixing box (full capacity of 165 litres) connected at the upstream part of the tank through a removable lock-gate (0.21 m wide and 0.70 m high). An electric-mechanical mixer was installed within that box to assure the full mixing of sediment mixture. The tank also had a dispersion zone (approximately 1.00 m length) in which the water (and flow) were drained after the experiment.

In all sets of experiments were used lock-exchange methodology characterized by the instantaneously release of the mixture (lock-gate opening) reproducing a catastrophic event on nature. As soon as the mixture entered into the channel, the dense flow was generated.

In order to measure the flow properties during the experiments, a group of equipments was installed within the tank. Four UHCM's (*Ultrasonic High-Concentration Meter*) were set along the vertical profile (at 1.0; 3.2; 6.4 and 10 cm from the bottom) to acquire time-series concentration data, whilst ten UVP's (*Ultrasonic Doppler Velocity Profiler*) of 2 MHz transducers were set along vertical profile (15 cm) to register time-series of velocity data. Both equipments were located at 340 cm from the gate. With both velocity and concentration data, the hydrodynamic properties were established for all flows such as: time series of velocity and concentration, mean vertical profiles, non-dimensional parameters for the head, body and tail zones.

Additionally, all flows were recorded with a digital video-camera placed on the side of the tank in order to evaluate the time series of geometric features of the current (see Fig. 1), such as: *the current height* ( $h_t$ ); *thickness of the body* ( $h_b$ ) defined as the height of the body not considering the mixing zone at the upper surface and; *thickness of the internal layer* ( $h_i$ ), which considers the interface layer created by the presence of a more concentrated zone near the bottom. The depositional properties (e.g. deposition rate) were also evaluated through the video images.

After the experiment, the ambient fluid was slowly drained and the final deposit properties (e.g. thickness, grain-size and mass balance) were measured (and/or sampled).

### 3. Rheology of mixtures

The rheology is the study of deformation and flow of matter and is a property of the fluid that expresses its behaviour under an applied shear stress. Through the rheological characterization of mixtures (water and sediment), it is possible to establish the relationship between shear stress and strain rate (shear rate), and consequently the coefficient of dynamic viscosity (and/or apparent) as well as the constitutive equations in terms of volumetric concentration and presence of clay.

In natural flows, the non-conservative condition of the sediment gravity flows, i.e. erosion and deposition during the movement, modifies the mechanisms of transport and deposition of particles within the flow (e.g. local concentration, size and composition of grains in suspension), which impact also their rheological behaviour.

Based on this, a rheological characterization of mixtures was carried out aiming to establish such property of the mixtures and verify its behaviour for different initial conditions. To do that, it was used a Rheometer device with two types of spindle (cone plate and parallel plate). For the tests, the mixtures were prepared following the same proportions of sediment used in the experimental work and also considering the same temperature ( $\sim 19^\circ\text{C}$ ). The rheogram - output data of the Rheometer consisting in the ratio of shear stress and strain rate - was compared to typical rheological models found in literature. The simplest rheological model of imposed stress ( $\tau_x$ ) related to strain rate ( $\delta u/\delta z$ ) is the *Newtonian* model (due to the definition of Newton's law of viscosity) and it can be expressed for two-dimensional flow in the  $x - z$  plane as:

$$\tau_x = \mu \frac{\partial u}{\partial z} \quad (1)$$

The equation (1) shows a linear relationship between the imposed shear stress and strain rate (gradient of deformation). As a consequence, the viscosity of the fluid or mixture (*coefficient of dynamic viscosity* -  $\mu$ ) is constant for all values of shear rate. Any deviation from linearity between the stress-strain curve converts the rheological property to non-Newtonian behaviours, which can be generally divided into four more groups: *plastics* in which there is no deformation of the flow until the critical initial stress (yield strength -  $\tau_0$ ) is overcome; *dilatant and pseudoplastic*, in which the deformation (strain rate) is expressed by a power law type (if coefficient of power law  $n > 1$  then the fluid is *dilatant* otherwise ( $n < 1$ ) is *pseudoplastic*) and; *Herschel-Bulkley* in which the fluids has a plastic behaviour (yield strength -  $\tau_0$ ) followed by a power law behaviour. The *Herschel-Bulkley* model can be expressed for two-dimensional flow in the  $x - z$  plane as:



$$\tau_{ap} = \tau_0 + K \left( \frac{\partial u}{\partial z} \right)^n \tag{2}$$

To non-Newtonian mixtures, the determination of viscosity (curve slope at the rheogram) is no longer direct, implying that for each value of gradient of deformation (strain rate) applied, there will be a different coefficient of dynamic viscosity. When this occurs, the viscosity is called *apparent viscosity of the fluid* ( $\mu_{ap}$ ) rather than the dynamic viscosity. From the results obtained with the rheometry tests, it was defined two distinct groups for the mixtures simulated in terms of different values of concentration and clay content: the Newtonian group of mixtures and the Herschel-Bulkley plastic group of mixtures (Fig. 5).

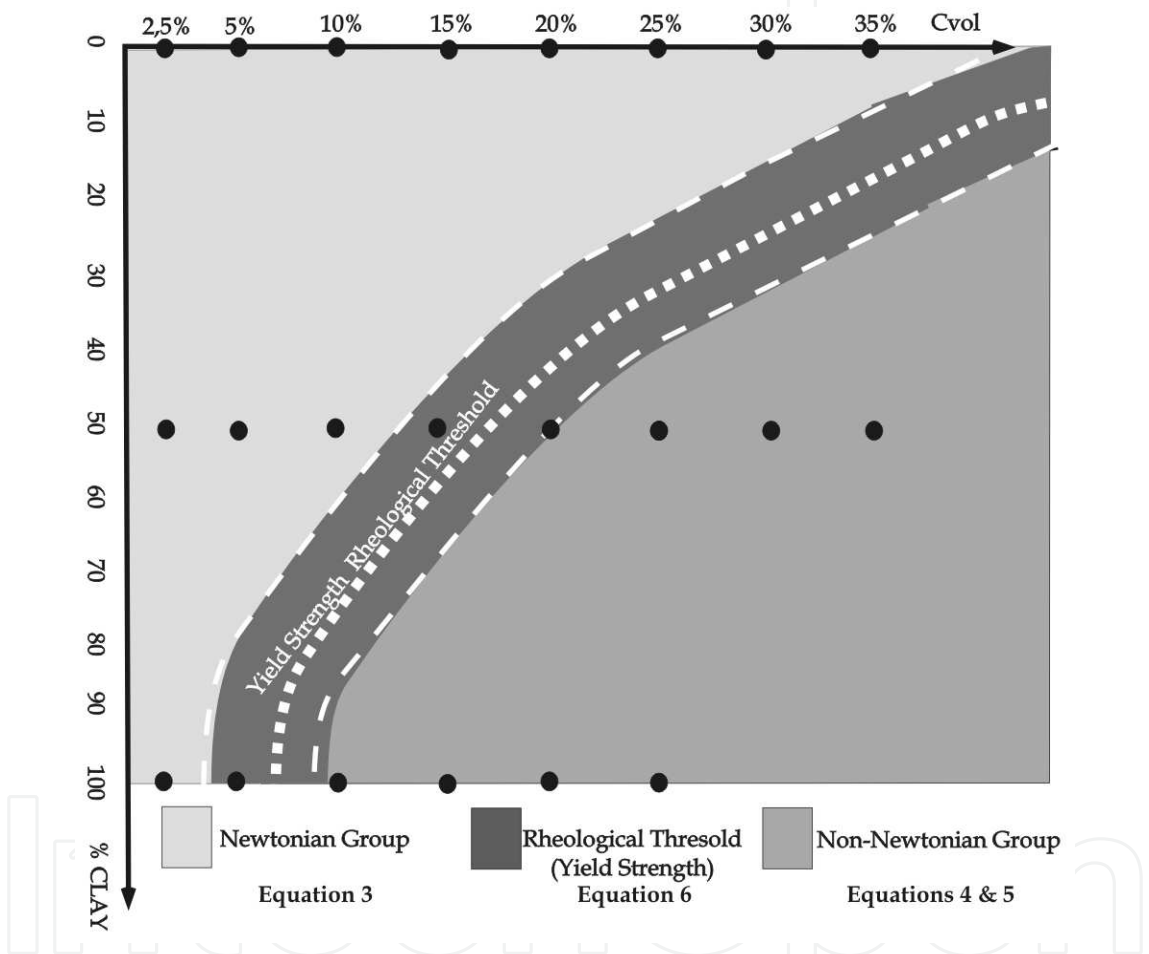


Fig. 5. Rheological characterization of the mixtures simulated and the constitutive equations in terms of volumetric concentration and presence of clay for each group.

For the group of Newtonian mixtures (above threshold line) it was possible to establish an empirical relationship (linear) between the values of dynamic viscosity with the volumetric concentration and clay presence, which allows properly assess the effect of viscosity on the hydrodynamic parameters for this group of mixtures (eq. 3). The coefficient values were similar to those found in literature for non-cohesive grain mixtures (e.g. Coussot, 1997; Einstein, 1906). The rheological characterization was carried out to the volumetric concentration of 35% only. Extrapolation to higher values must be handled carefully (see Coussot, 1997; Wan & Wang, 1994).

$$\frac{\mu}{\mu_0} = 1 + C_{vol} (2.24 + 0.44 \%Clay) \quad (3)$$

The threshold line represents the transition from Newtonian to non-Newtonian behaviour (plastic) and can be represented by the occurrence of yield strength. Clearly, there is not a unique value representing this change of rheological behaviour. A transition interval must be considered (dashed line around the threshold) to more accurate analysis. In addition, different composition of clay may move the position of the curve, for instance; the threshold of montmorillonite shows similar shape. However this curve of yield strength (high values for this particular type of clay) is moved into the top-left of the diagram.

For the group of Herschel-Bulkley plastic mixtures (high concentration and more presence of clay - below the threshold line) the constitutive equations were empirically determined (eq. 4, 5) correlating the apparent viscosity, the clay content in the mixture, the bulk concentration of the mixtures and, the gradient of deformation (strain rate) for this group of mixtures.

$$\frac{\mu_{ap}}{\mu_0} = \left[ 1.39 e^{(31 C_{vol})} \left( \frac{\partial u}{\partial z} \right)^{(0.24 - 1.8 C_{vol})} \right] \cdot C_{clay} \quad (4)$$

where

$$C_{clay} = 0.0016 e^{(8.7 \%Clay)} \frac{\partial u}{\partial z}^{(0.59 - \%Clay)} \quad (5)$$

It was also established an empirical relationship to yield strength in terms of the volumetric concentration and the presence of clay in the mixture.

$$\tau_i = 0.00104 e^{(2790 \%Clay C_{vol})} \quad (6)$$

#### 4. Experimental results

The rheological characterization (rheometry) has classified the mixtures into two distinct groups as it was illustrated in Fig. 5. Based on that approach, all data and results obtained through experimental work were compared in order to establish groups with similar properties. A total of 15 parameters divided into seven categories were used to fully characterize and distinguish each group: geometry, rheology, analysis of mean vertical profiles, time-series of data, internal dynamics of the flow, depositional features and, non-dimensional parameters as seen in Fig. 6.

After applying this method of analysis, it was possible to identify six regions (or groups) of similar sediment gravity flows generated experimentally. Each one has typical properties and characteristics in terms of rheology, geometry, hydrodynamic and depositional processes along time and space. Moreover, the relationship with initial properties (concentration and clay content) demonstrates the cause-consequence of the experiments (from source to deposit) and the entire dynamic involved. The Fig. 7 illustrates this diagram-phase with delimited boundaries amongst the regions.

Each region properties will be completely described below from non-cohesive dominated flows (regions I, II and III) to cohesive dominated flows (regions IV, V and VI). The averaged vertical profiles will be discussed apart (item 4.6).

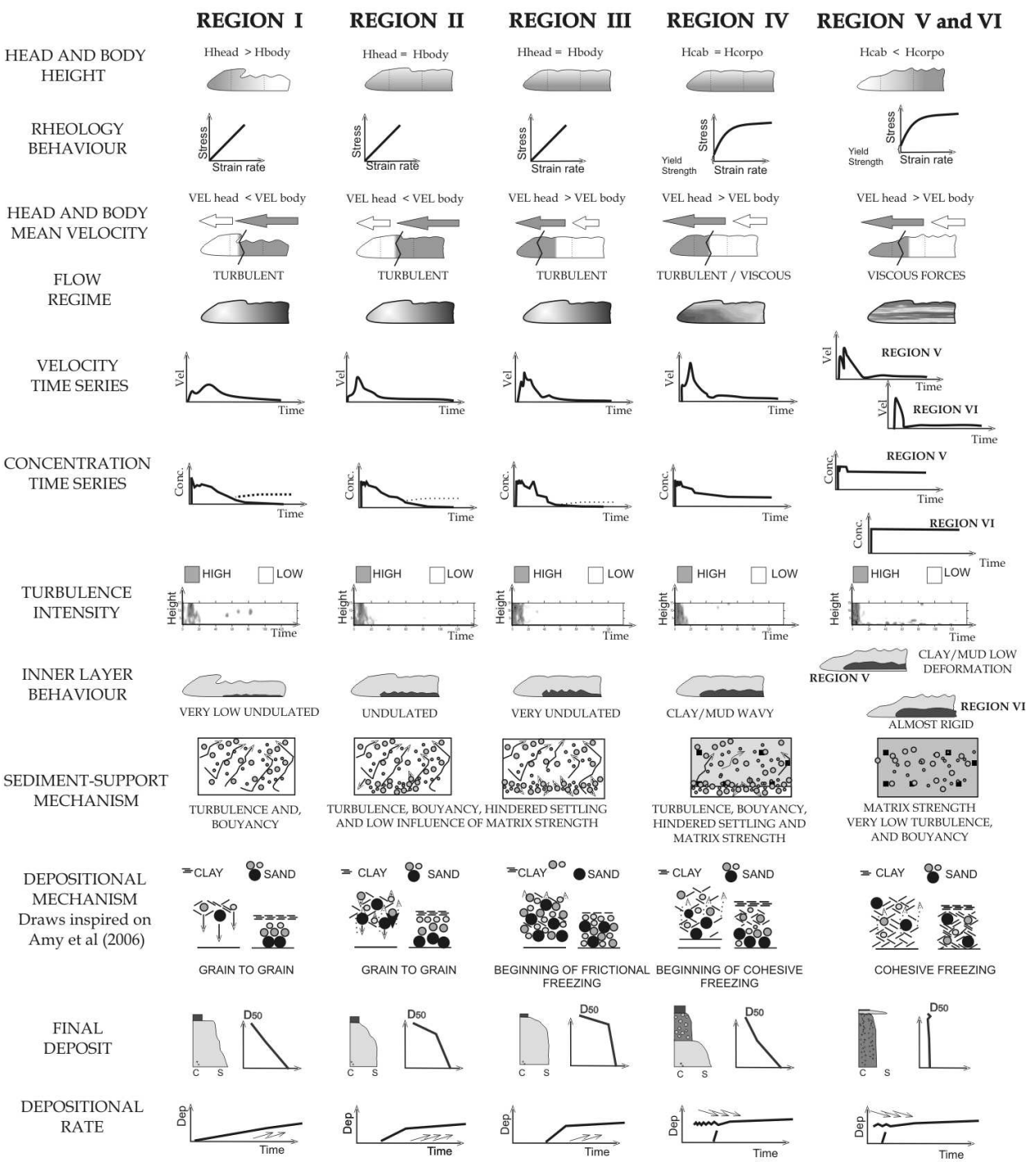


Fig. 6. Results obtained through the experimental simulations

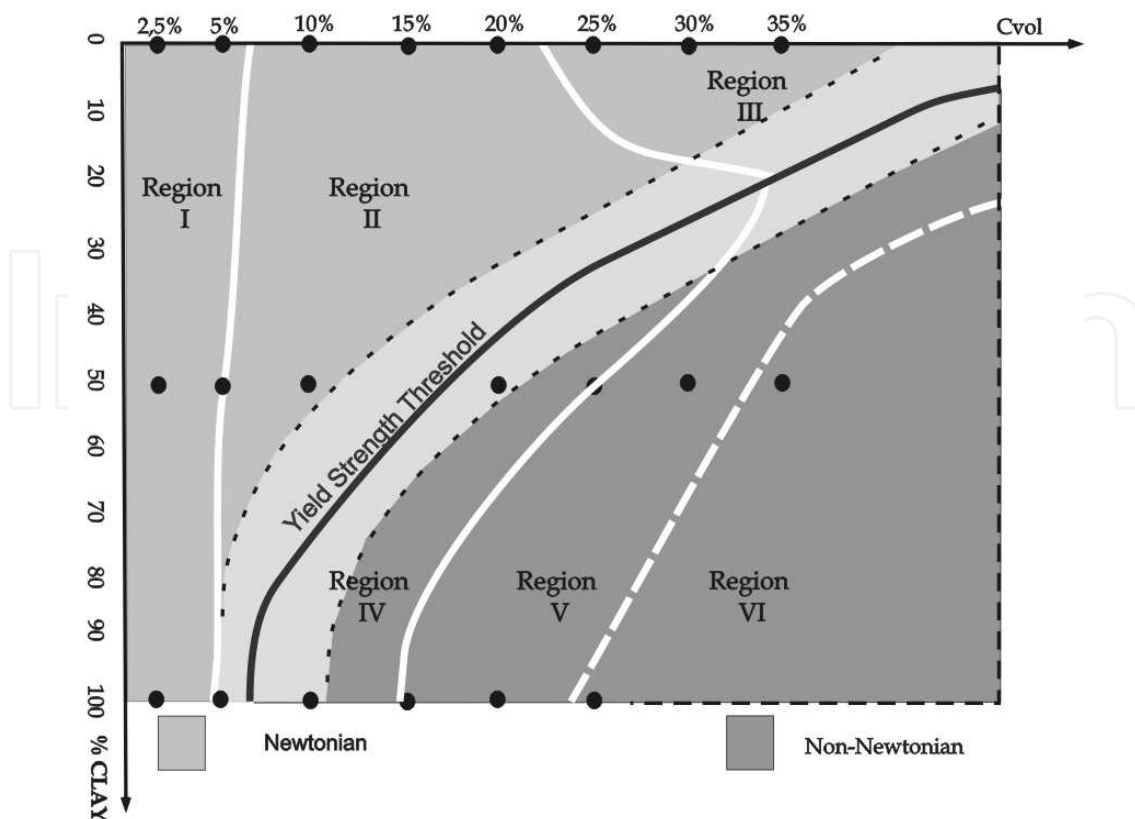


Fig. 7. Six regions (or groups) of similar sediment gravity flows generated experimentally

#### 4.1 Region I - Turbidity currents like sediment gravity flows

Sediment gravity flows generated considering the properties of the region I (Newtonian, low-volumetric concentration ( $< 5\%$ ) regardless of the amount of clay) reproduces a classic behaviour of turbidity currents widely discussed in the literature (Kneller & Buckee, 2000; Middleton, 1966; Simpson, 1997). The current accelerates (waxing flow - Kneller, 1995) due to the buoyancy flux with clearly defined head at the front. The thickness of the head is greater than the body, indicating the flow undergoes a large resistance of the ambient fluid and also from gravitational forces acting over the body. As consequence, a large billow (shear vortex) takes place behind the head (high mixing zone).

The body presents the peak of velocity and after this point the flow starts to decelerate gradually (waning flows - Kneller, 1995). Concomitantly, the concentration of sediment within the flow follows the velocity behaviour. In the head, sediments are held in suspension by virtue of the high-turbulence intensity (no depositional zone) and then, the suspended sediments start to settle (fall out) with the decrease in velocity. The current becomes diluted and finally there is only the sedimentation of finer particles by decantation (very long time for cohesive particles because of low settling velocity).

In these currents the main mechanism of grain support is turbulence (inertial forces) with high Reynolds numbers along the entire current (despite the low concentration of mixtures) except for the final stages of the flow (tail). The evaluation of the turbulent intensity (*root mean square* - RMS) shows that turbulence occurs mainly in the head and particularly in the vortex generated behind the head whilst in the body, turbulence occurs around shear layer (mixing zone). Along the vertical profile there was absence of high RMS values near the

bottom, which may explain the initiation of the deposition just after the passage of the front. For the flows of this region, the presence of cohesive sediments at low concentrations ( $< 5\%$ ) implies in no significant changes on the flow behaviour.

During the flow movement, the main mechanism of deposition was by individual particles (grain-to-grain) falling out from suspension by gravity (decelerating flow). Consequently, the dissipation of turbulence caused the lost of sediment-transport capacity of the flow and the grains segregated naturally, i.e. the coarse grains (high setting velocity) were deposited first followed by fine grains and then by colloidal particles (after the stop indeed). As a result, the deposits generated normal gradation (decreasing mean grain size towards to the top - fining upward). For the flows containing clay in suspension, the deposit is characterized by a non-cohesive layer of grains near the bottom with a layer of clay (as a resulted of settling) at the top. The contact between the non-cohesive and cohesive grains is very sharp, clearly indicating different stages of deposition. Despite the fact that clay may form flocs, due to the cohesion of their particles, there was no evidence of the formation of large flocs. The depositional rate for this class of flows was linear (deposit thickness increased at constant rate) starting just after the passage of the head.

#### 4.2 Region II

The Newtonian sediment gravity flows originated by the increase in concentration and the presence of clay (around 50%) showed differences in the properties of the flow dynamics and deposition. Both velocity and buoyancy flux increased in the flow causing a decreased in the head height. As a result, the average velocities of the body and head were almost identical, showing that buoyancy forces present in the head are in balance with gravitational forces. Yet, the head of the current is slightly higher then the body and is characterized by intense mixing zone. The main difference comparing with region I can be noticed after the peak of velocity in the body, since the flow rapidly decelerates reaching low values of velocity until completely stopped (tail). The quick deceleration is related to formation of an inner layer of grains more concentrated near the bottom. For a short time the flow becomes stratified (bipartite) changing the velocity and concentration profile instantly and implying in different mechanisms of deposition.

The sediment-support mechanism of the non-cohesive flows (low content of clay) is driven by the turbulence of the flow (in the head), Kelvin-Helmholtz instabilities behind the head and along the mixture layer at the upper and the bottom surfaces. The high values of turbulence intensity were measured throughout vertical profile explaining a period of no deposition at early stages of the flow. Also, the concentrated near-bed layer (mainly non-cohesive) is characterized by high turbulence intensity and its internal undulations are closely related to instabilities at the upper surface.

The flows generated from experiments adjacent to rheological threshold in Fig. (7), the increase of amount of clay and/or concentration caused a decrease in turbulence intensity. Also, not only the turbulence plays a key role on these flows but also the influence of the matrix strength and cohesive interaction of the grains started to become relatively significant. This fact is reflected on the behaviour of near-bed layer (mainly cohesive) which is characterized by undulations and deformations, although not as considerable as those presented by pure non-cohesive flows.

The mechanism of deposition in such flows differs from region I. Besides the grain-to-grain sedimentation caused by dissipation of the turbulence intensity (typical behaviour of flows



next to boundary between regions I and II), other depositional processes start to play in the flows regarding the amount of clay in the mixture.

In non-cohesive flows, the sediment in suspension settled down creating a concentrated near-bed layer that was constantly fed by sediments from the top (fall out). As consequence, the space between grains became more restricted causing rapid deposition of sediments (high depositional rate in the first stages of the flow where there was insufficient time for the natural segregation of the grains). Hence, the deposit generated *partially graded beds*, i.e., massive (coarse size) deposits at the bottom followed by fining upwards particles on the top (final stages of flow with low depositional rate).

Despite the presence of clay in the mixtures gives the impression to modify the mechanism of deposition of these currents, again, for this group of experiments the deposits show a clear division between the non-cohesive grains (at the bottom) and cohesive grains (at the top).

#### 4.3 Region III

The region III corresponds to Newtonian flows with high-concentration and low presence of clay (up to maximum of 20%). The hydrodynamics followed the processes described before (region II), considering the higher values of velocity (amongst all regions) and also the flux of buoyancy, which does not allow the grains settled down in the early stages of the flow. The magnitude of forces acting over the head (mainly buoyancy) and over the body (mainly gravitational) was similar reducing the head height. Once more the flow generates a very wavy concentrated layer close to the bottom, creating a bipartite flow which caused sudden deposition (high-depositional rate) of large amount of sediments. Then, the diluted current flows over the bed previously deposited (low-depositional rate).

The support mechanism of grain in these flows is basically turbulence generated at the head (high values of RMS) as well as the upper and lower surfaces. However, additional sediment-support mechanisms as hindered settling and dispersive pressure may occur within the concentrated near-bed layer (mainly non-cohesive). On the other side, the mechanism of deposition for these flows represents an evolution of the processes described in region II. Since the suspended load of sediment becomes progressively concentrated towards the bottom, the continuous supply of the grain from the top (fall out) compress the inner layer reducing space for grains to move. At this point, there is a rapid deposition of grains. This process may be a first signal of frictional freezing, where non-cohesive grains settle quickly (collapse) without segregating grains by size. As a result, deposit is partially graded; being massive graded near the bottom and normally graded (fining upward) on the top.

#### 4.4 Region IV

The flows classified as region IV are non-Newtonian, which consequently leads to changes in hydrodynamic properties, such as sediment-support mechanism and depositional processes, mainly because of the yield strength.

In this class of flows dominated by cohesive particles, the hydrodynamic processes are closely related to the region II. The head of the current is the local of high velocity, turbulent intensity and mixing, whilst the viscous forces play a significant role on the body causing deceleration and then, the early stage of deposition. It was also verified the formation of a concentrated layer (mainly dominated by clay) at the bottom. The presence of this deformable clay/mud near-bed layer is followed by a constant value of inner concentration.

The sediment-support mechanism is influenced by the content of clay once the turbulence is damped within the current (being only verified in the head of the flow). The cohesive matrix begins to act internally changing the hydrodynamic behaviour of the current. The buoyancy of the interstitial fluid (water and clay) and pore-pressure also contribute to keep the grains in suspension inside the clay/mud near-bed. This behaviour differs from Newtonian non-cohesive flows (regions II and III). In region IV, the concentration has not yet reached the gelling concentration for cohesive mixtures (Winterwerp, 2002).

During the flow, it was possible clearly identify the shear-like flow near the bed and plug-like flow above that, which is dominated by viscous forces acting on the flow. However, the flow can not be classified as completely laminar, since spots of turbulence (high intensity) can be generated within this layer. Also, in the plug-like flow, fluid shear stress is lower than yield strength of the mixture, generating an instantaneously mass deposit (cohesive freezing). As it occurs suddenly, there is no segregation (selection) of the grains. On the other side, the shear stress at the bed is higher enough to allow the settled of non-cohesive sediments. As a result, the final deposit is divided into three distinct depositional layers: low-content clay (~ 5%) bottom layer (shear-like flow); an intermediate ungraded matrix of sand and clay/mud layer (plug-like flow) and; a clay dominant layer on the top (tail and settling deposition).

#### **4.5 Region V and Region VI - Debris flow like sediment gravity flow**

Regions V and VI have very similar behaviour with high concentration and high amount of cohesive material (Herschel-Bulkley rheological model). This region represents the other extreme of sediment gravity flows evolution and their transformations.

The hydrodynamic of the current was influenced by the clay content presenting a strong waxing flow-phase (high-turbulence intensity only at the head) and abrupt deceleration, after the arrival of deformable clay/mud near-bed layer (for Region V) and practically not undulating/deformable (for region VI). The plug-like flow in the body induced cohesive freezing, in which a large amount of sediments are deposited in few seconds (high-depositional rate). In this region, the content of clay in the mixture at high concentrations is influenced by the gelling concentration. According to the literature, this occurs at concentrations of clay between 80 and 180 g/l, equivalent to a solid volume fraction of 0.03 and 0.07 (Whitehouse et al., 2000; Winterwerp, 2001, 2002). The mixtures simulated in the regions V and VI correspond to this range of values. Therefore, the cohesive forces acting on these deposits are transmitted to all mass deposited and not only to each single particle causing a thick ungraded chaotic deposit.

The sediment-support mechanism is highly influenced by the increased of apparent viscosity of the mixture and matrix strength which is induced by electrostatic interactions of clay particles. Thus, turbulence is damped throughout the flow, with local spots of high-turbulence intensity close to the bottom (high values), as well as at the interface between the deposit generated by clay/mud near-bed layer and the remaining flow (body and tail). This final stage of the flow generates a normally graded deposit (coarse-tail grading on the top) associated to the mechanism of deposition described in the region I (turbidity currents like flows).

#### **4.6 Mean vertical profiles**

Based on the experimental results, Fig. (8) illustrated the idealized pattern for each region concerning the average velocity, concentration and sediment flux vertical profiles.

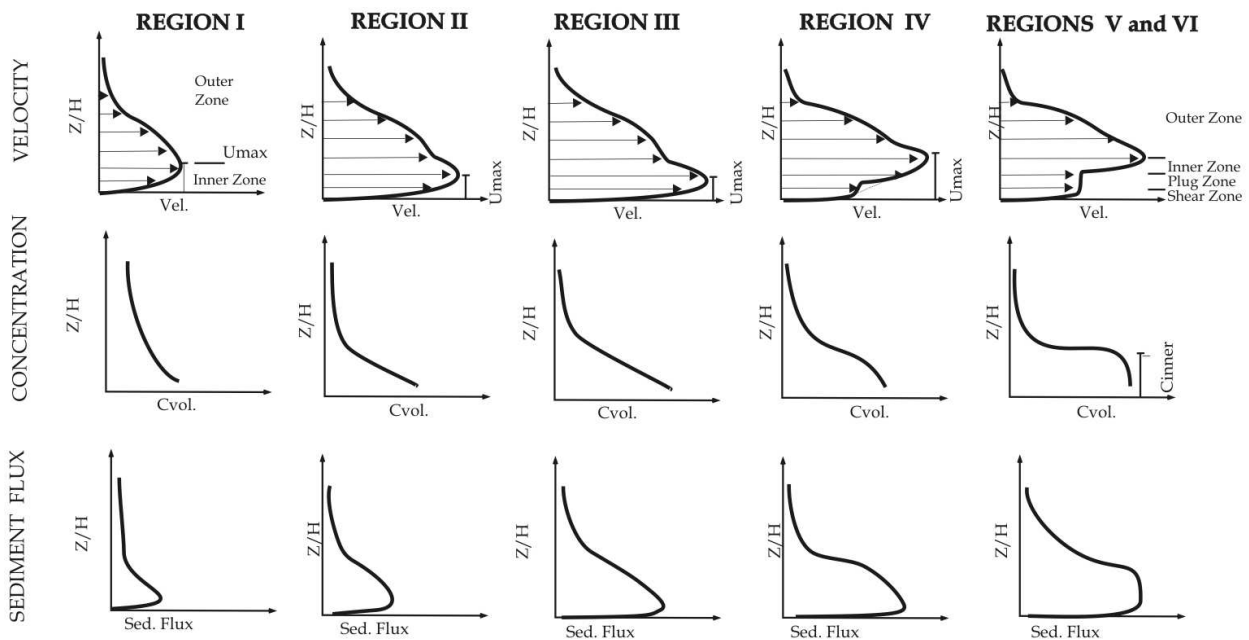


Fig. 8. Mean vertical profiles of velocity, concentration and sediment flux for the six regions of sediment gravity flows.

4.6.1 Velocity profiles

Concerning the flows classified as Newtonian (regions I, II and III), the velocity profile presented the classical behaviour of turbidity current (see description section 1.1) with a maximum velocity point located at some distance from the bottom and two distinct zones: an inner zone near the wall and an outer zone up to the top surface (Fig 8, top-left). Applying the model developed by Michon et al., (1955) and modified by Altinakar, (1988) it was possible to establish analytical equations for non-dimensional velocity profiles in terms of initial concentration of the flow.

The model consists in a relationship between a non-dimensional velocity and geometry parameters and also separates the velocity profile in two zones (the threshold is height of maximum velocity -  $h_m$ ). The equations below present the results of applied methodology for the inner zone ( $z < h_m$ ) including the parameters fitted for this group of experiments.

$$\frac{u}{U_{max}} = \left( \frac{z}{h_{max}} \right)^{0.4} \tag{7}$$

And for the outer zone ( $z > h_m$ ) is,

$$\frac{u}{U_{max}} = e^{\left[ -2.7 \left( \frac{z-h_m}{h_t-h_m} \right)^{1.9} \right]} \tag{8}$$

Those equations can be applied to a wider range of currents with different behaviours as the first approximation of the non-dimensional velocity profile for Newtonian sediment gravity

flows. However, in order to extrapolate the results to natural fields, it must take into consideration the maximum velocity value and its location within the current.

For the flows classified as non-Newtonian (regions IV, V and VI) the velocity profile changes drastically and can be divided in four zones (Fig. 8 top-right): the *shear-like flow* zone (near the bottom), strongly influenced by viscous sublayer; the *plug-like flow* zone: occurs when the value of the shear stress is lower than yield strength; and the *other two zones* from the remaining diluted current (similar to Newtonian flows described above). The first two zones involve the evaluation of the shear stress at the wall (viscous sublayer) and the thickness of the plug. For the last two zones above the plug-like flow the model of Michon et al., (1955) can be adjusted adding the plug-like flow velocity and its thickness.

The velocity profiles measured for the high-density currents were similar to those cited by (McCave & Jones, 1988; Postma et al., 1988, Talling et al., 2007). To express these profiles in terms of equations require a detailed analysis of stress distribution along the vertical profiles (to establish the shear zone and plug zone) as well as the estimative of the thickness of the near-bed layer (inner flow). In nature those parameters are not easily estimated. The detailed evaluation of these parameters can be found in Manica, (2009).

#### 4.6.2 Concentration profile

The mean concentration profile measured in the experiments show the transition between the six regions of sediment gravity flows (Fig. 8). For flows classified as Newtonian (regions I, II and III) the profile is practically more invariable along the vertical (region I) with a slight increase (creating an inflexion point) at the concentration values near the bottom. The curve is similar to an exponential trend (regions II and III), corresponding typical profiles of open-channel flows (e.g. rivers). An empirical exponential law can be fit in such type of curves considering non-dimensional parameters defined as: local concentration divided by concentration measured at 5% of the total height of the flow (concentration of reference -  $C_r$ ); and the distance from the bottom divided by total height of the current ( $z/h_t$ ). The equation fitted for the experimental results is expressed by

$$\frac{C(z)}{C_r} = 1.22 \cdot e^{\left(-4.0 \frac{z}{h_t}\right)} \quad (9)$$

Considering the non-Newtonian sedimentary gravity flows (regions IV, V and VI), the vertical profile of concentrations is strongly influenced by the clay/mud inner layer, which generates high-levels of concentration and, practically stratified the profile into two regions (threshold is the inner layer thickness - see Fig. 1). In terms of analytical adjustment of these peculiar curves, the definition of this threshold point is crucial, once it can be presumed for  $z < h_i$  that concentration assumes the value of concentration of reference. Above the clay/mud inner layer, equation (9) can be applied.

The methodology presented here to obtain the non-dimensional concentration profiles (Fig. 9) was straightforward in order to simplify at maximum the input parameters. Methodologies found in literature such as (Graf & Altinakar, 1998, Parker et al., 1987) were tested and applied showing very similar results.

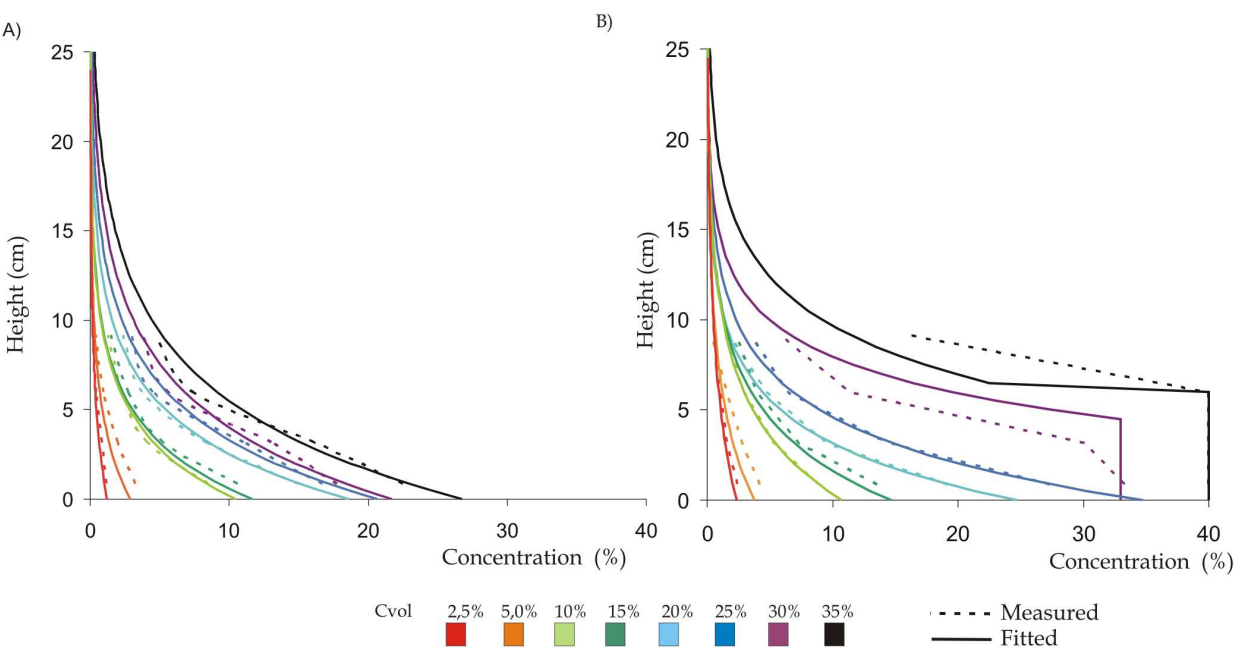


Fig. 9. Concentration profiles measured and fitted curves for the two groups of sediment gravity flows simulated: a) regions I, II and III; b) regions IV, V and VI.

4.6.3 Reduced Flux of Sediment

The evaluation of the reduced flux of sediments gives the idea of the mass conservation during the flow, since velocity, concentration and, initial properties of the flow (reduced gravity) are taken into account (eq. 10). Through the evaluation of this parameter, it is possible to check which zone within the flow the sediments are being transported as seen in the experimentally-derived profiles in Fig. 8.

$$S_{\text{Flux}} = g \cdot \left( \frac{\rho_m - \rho_a}{\rho_a} \right) \cdot C_{\text{vol}} \cdot h_{\text{mean}} \cdot u_{\text{mean}}$$

(10)

The differences among all classes of sedimentary gravity flows simulated were evidenced, particularly, the influence of the cohesive particles (non-Newtonian regions), which implying in a great amount of sediments at the bottom of the current.

5. Spatial evolution of the sediment gravity flows

The limitations of the simulations in terms of the length of the tank do not allow a complete study on spatial variability of the sediment gravity flows from their origin to the final deposit. Nonetheless, the full characterization of the main parameters involved in the flow such as time series, vertical profiles, rheology, deposition and so on, may be applied in order to extrapolate the results to natural ambient. Based on that, a detailed spatial analysis was accomplished and the flow evolution for each region will be described below.

Concerning the flows from regions I and II, both concentration and presence of clay increased sediment capacity of transport of the flow, indicating the current could flow further. At the early stages (near the source) the gravity flow is more concentrated with high buoyancy flux and high-turbulence. As the flow propagates downstream, the hydrodynamic



processes (e.g. entrainment of ambient water at the upper surface) and depositional processes (e.g. deposition of sediment over time and space) take place, transforming the inner properties of the flow. As a result, the current become more diluted due to deceleration of the flow, losing their capacity of transport (grains settled down) and then, tend to stop. The final deposit shows coarse grains in the proximal areas, due to deposition by gravity (high-settling velocity) and a gradually grain size thinning towards to downstream (low-settling velocity). The Fig. 10 illustrates a model of propagation for flows from region I to region II, also considering their transition points.

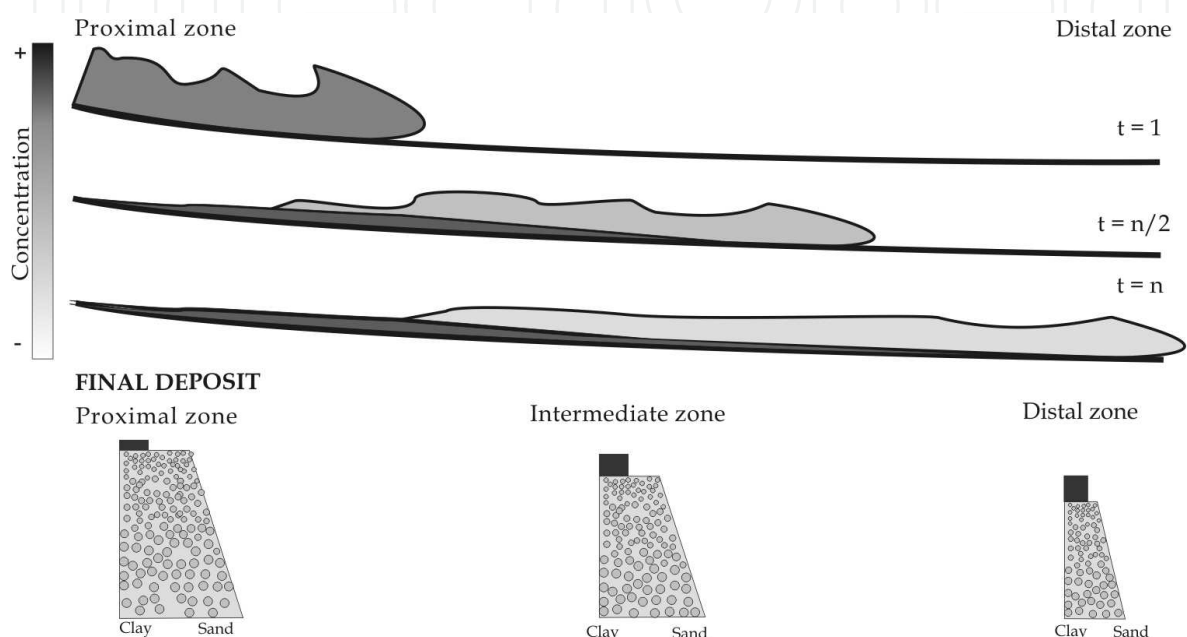


Fig. 10. Spatial evolution scheme of the sediment gravity flow for regions I and II.

In the flows characterized by high concentration and high content of clay (regions II and III) the hydrodynamic properties of the flow change during the run by virtue of the presence of concentrated near-bed layer. The suspended sediment rapidly settled down after the formation of this concentrated layer, causing a reduction in buoyancy flux. As consequence, the remaining diluted current is not able to travel further. This process occurs mainly in the proximal and intermediate zones, where the final deposit is, basically, massive graded. After this zone, the deposits were mainly generated by settling of the grains (gravity) up to distal zone (Fig. 11).

The spatial evolution of the deposit for non-Newtonian mixtures (regions IV, V and VI) showed a distinct behaviour. The increase of flow sediment capacity of transport by reason of high concentration and high presence of clay was counter-balanced by viscous forces, which dominated the flow dynamics and consequently, the generation of the clay/mud near-bed layer. Thus, the bulk of sediment from regions IV, V and VI was not able to travel long distances. Within the plug-like flow, the shear stress of the flow was not enough to prevail over the yield strength of the mixture. As a result, the deposit showed a great quantity of sediment in the proximal zone, whilst only a remaining diluted current flows (with more fine particles) moving to distal zones. The Fig. 12 illustrates this idealized model. The main difference between the idealized transition models of evolution to non-Newtonian sediment gravity flow regards the dynamic of the clay/mud near-bed layer and the final

deposit. From region IV to V, a concentrated inner layer presents a high deformation and undulation over time, with a shear-like flow near the bottom and a plug-like flow above (generating the three layer deposit commented on section 4.4). On the other side, from region V to VI (Fig. 13), the near-bed layer is practically a solid mass of mixture flowing downstream, generating a thick clay/muddy deposit at proximal zone.

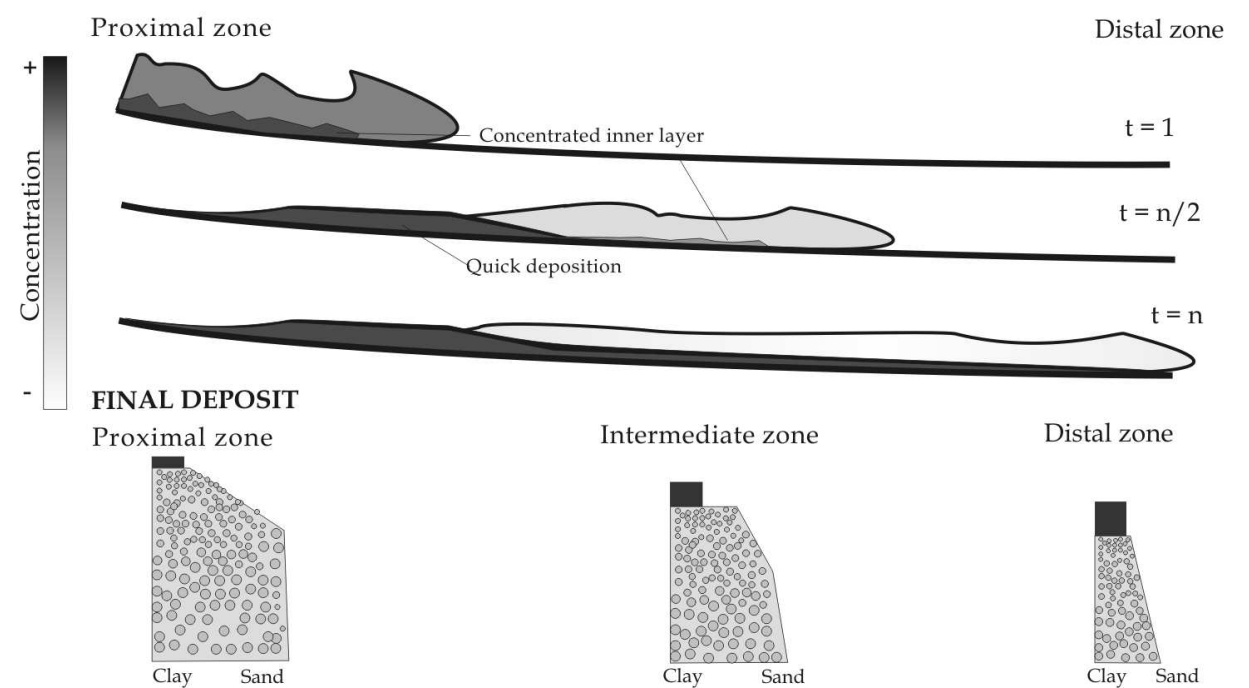


Fig. 11. Spatial evolution scheme of the sediment gravity flow for regions II and III.

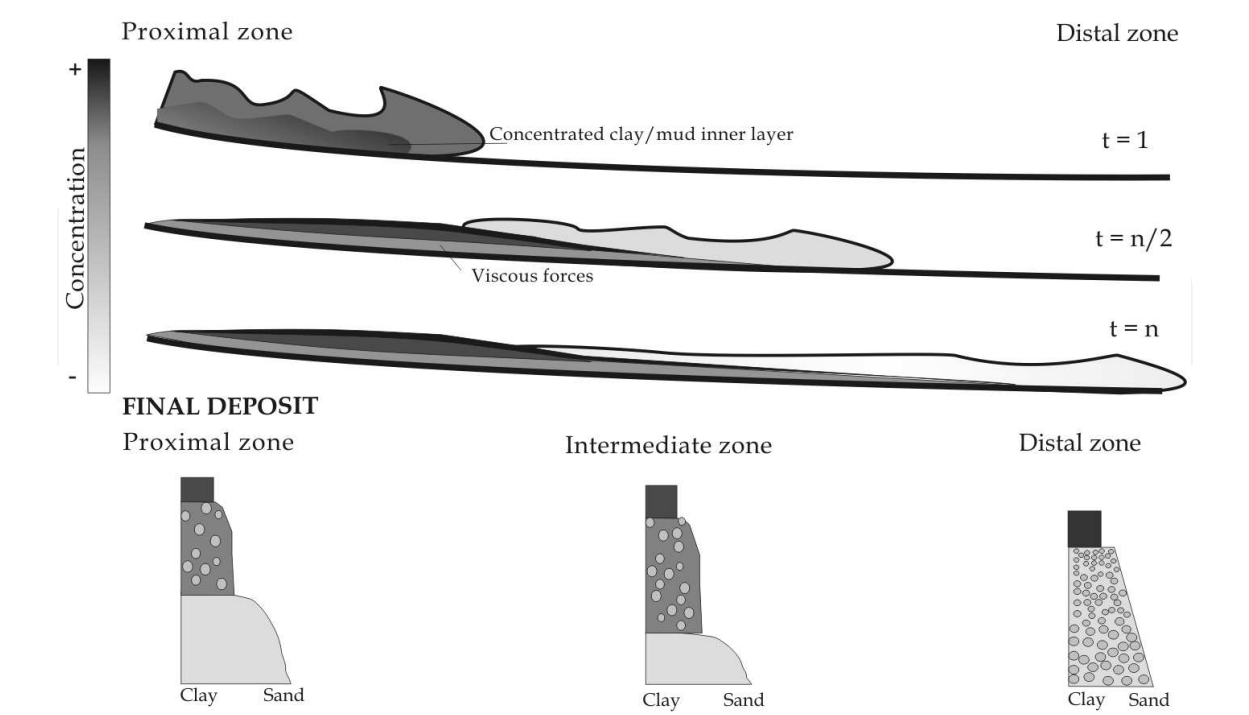


Fig. 12. Spatial evolution scheme of the sediment gravity flow for regions VI and V

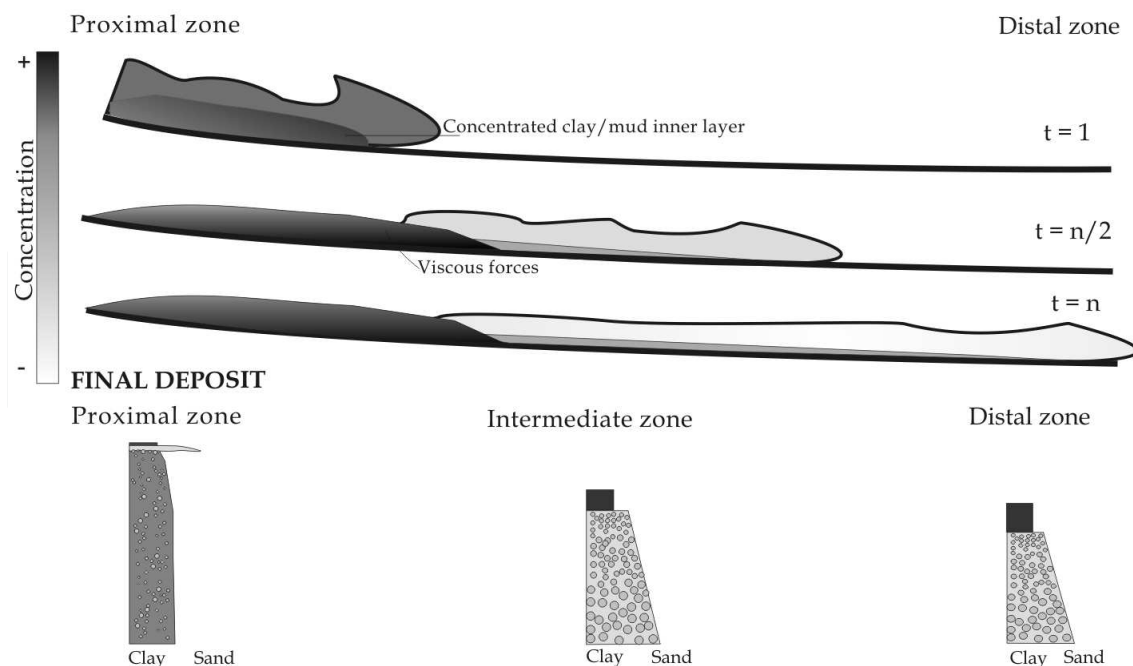


Fig. 13. Spatial evolution scheme of the sediment gravity flow for regions V and VI

## 6. Conclusion

This chapter presented an experimental study of sediment gravity flows in which six types of flows were distinguished based on a comparison of hydrodynamic, depositional and rheological properties. A phase diagram was created, showing the boundaries between these flow types in terms of rheological behaviour, bulk volumetric concentration and clay concentration. The main characteristics of the flow types are summarized below:

Type I: Low density flow; Newtonian; grains supported by upward component of turbulence; no hindered settling; segregation of grains and normally graded beds; Type II: Newtonian; grains supported by turbulence; turbulent flow with gently undulating high-concentration near-bed layer; partial hindered settling and partial size segregation forming partially graded beds; Type III: Newtonian; fully turbulent flow with strongly undulating high-concentration near-bed layer; hindered settling resulting in rapid deposition and generation of partially graded beds; Type IV: non-Newtonian (plastic); viscous flow; formation of plug and shear flow (mud layer close the bottom); viscous forces cause freezing of the flow and forming graded beds of muddy sand and; Types V and VI: non-Newtonian (plastic); viscous flow with thick mud layer; grain support by matrix strength; weakly undulating internal mud layer (type VI show no undulations); cohesive freezing forms an ungraded muddy sand with coarse-tail grading on top.

The six types of flow/deposits classified represent the transition between the two most known types of sedimentary gravity flows: from turbidity currents (low-concentration, low clay and Newtonian behaviour) to debris flow (high-concentration and high clay content and non-Newtonian behaviour). The experimental study allows the comparison and extrapolation of the results obtained from physical model to natural environments. However it must be considered the experimental simplifications adopted. Apart from that, the rheological properties of mixtures and some hydrodynamic (e.g. cohesion effects) and depositional (e.g. settling velocity) properties are scale-independent and can be applied for further interpretation.

The experiments simulated a single catastrophic event and do not consider a continuous sediment supply from rivers (for instance, plumes and hyperpycnal flows among others) which can change some properties of the flow along time and space. Moreover, the limit of maximum value of volumetric concentration was 35% by volume. In this case, regions III (see Amy et al., 2006) and region VI (see e.g. Hampton, 1972; Ilstad et al., 2004; Marr et al., 2001; Mohrig et al., 1999; Mohrig & Marr, 2003) were left with an open boundary to further experiments and perhaps the creation of a complementary experimental-derived classification of sediment gravity flows.

7. Nomenclature

%Clay	clay content in the mixture (%)
$C_r$	concentration of reference (%)
$C_{vol}$	volumetric concentration (%)
$C(z)$	volumetric concentration at the point $z$ (%)
$\partial u / \partial z$	strain rate (1/s)
$g$	acceleration of gravity (m/s <sup>2</sup> )
$h_b$	body height (m),
$h_h$	head height (m),
$h_i$	inner layer thickness (m),
$h_m$	height of the point of maximum velocity (m),
$h_{mean}$	mean current height (m),
$h_t$ or $H$	overall height of the current (cm),
$K$	consistence coefficient
$n$	power law coefficient
$S_{flux}$	sediment flux (m <sup>3</sup> /s <sup>3</sup> )
$u$	current velocity (m/s),
$U_{max}$	maximum current velocity (m/s),
$u_{mean}$	mean current velocity (m/s),
$Z$ or $z$	distance to bottom (cm)

Greek letters

$\mu_o$	coefficient of dynamic viscosity of pure water (Pa.s)
$\mu$	dynamic viscosity coefficient (Pa.s)
$\mu_{ap}$	apparent viscosity coefficient (Pa.s)
$\rho_a$	density of ambient fluid (kg/m <sup>3</sup> )
$\rho_m$	density of mixture (kg/m <sup>3</sup> )
$\tau_i$	yield strength - critical shear stress (Pa)
$\tau_0$	shear stress at the bottom (Pa)
$\tau_{lam}$	laminar component of shear stress (Pa)
$\tau_{turb}$	turbulent component of shear stress (Pa)
$\tau_x$	shear stress (Pa)

8. Acknowledgement

A grateful thanks to: CNPq - Brazilian National Council for Scientific and Technological Development - to support my PhD “sandwich” program at University of Leeds; the head of

NECOD – Density Currents Research Center, IPH/UFRGS - Professor Rogério D. Maestri; to Professor Ana Luiza de O. Borges and professor Jaco H. Baas for their support and also to my colleagues Eduardo Puhl and Richard E. Ducker.

## 9. References

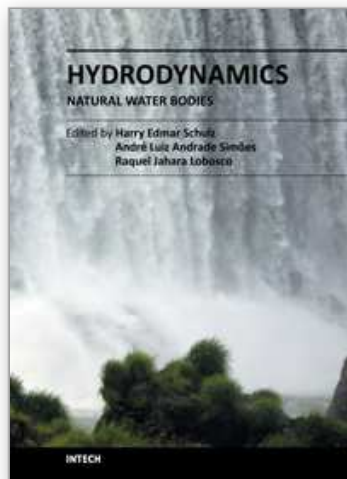
- Amy, L. A., Talling, P. J., Edmonds, V. O., Sumner, E. J. & Leseur, A. (2006) An experimental investigation on sand-mud suspension settling behaviour and implications for bimodal mud content of submarine flow deposits. *Sedimentology* Vol.53, pp. 1411–1434, ISSN 0037-0746
- Altinakar, M. S. (1988). Weakly depositing turbidity currents on small slopes. PhD thesys à Ecol. Pol. Fed. Lausanne.
- Baas, J.H.; Kesteren, W.V.; Postma, G. (2004). Deposits of depletive high-density turbidity currents: a flume analogue of bed geometry, structure and texture. *Sedimentology*, v51, pp. 1053-1088 ISSN 13653091 |
- Bouma, A. H. (1962). *Sedimentology of some flysch deposits: a graphic approach to facies interpretation*. Amsterdam. Netherlands
- Britter, R. E.; Simpson, E. J. (1978). Experiments on the dynamics of a gravity current head. *Journal of Fluid Mechanics*, Vol. 88, pp. 223-240. ISSN: 0022-1120.
- Coussot, P. (1997). *Mudflow Rheology and Dynamics*. Taylor & Francis. ISBN 905410693X.
- Einstein, A. (1906) Investigations on the theory of the Brownian movement (from the *annalen der physik*, Vol. 4), No. 19, pp. 289-306
- Elisson, T.H.; Turner, J. S. (1959). Turbulent entrainment in stratified flows. *Journal of Fluid Mechanics*, Vol. 6, pp. 423-448 ISSN: 00221120
- Fischer, R. V. (1983). Flow transformations in sediment gravity flows. *Geology*, Vol. 11, pp. 273-274, ISSN 0091-7613
- Gani, M. R. (2004). From Turbid to Lucid: A straightforward approach to sediment gravity flows and their deposits. *The Sedimentary Record*. September, 2004, Vol. 2, No. 3, pp. 4-8.
- Graf, W. e Altinakar, M. S. (1998). Turbidity currents, In: *Fluvial Hydraulics: Flow and Transport processes in channels of simple geometry*. W. H. Graff, (Ed.) 468-516, Jonh Wiley e Sons, ISBN: 978-0-471-97714-8 New York- US.
- Hampton, M.A. (1972). The role of subaqueous debris flow in generating turbidity currents. *Journal of Sedimentary Petrology*, Vol. 42, No 4, pp. 775-793 ISSN 0016-7606
- Iltad, T., Elverhøi, A., Issler, D., & Marr, J. (2004). Subaqueous debris flow behaviour and its dependence on the sand/clay ratio: a laboratory study using particle tracking. *Marine Geology*, Vol. 213, pp. 415–438, ISSN 0025-3227
- Kneller, B. (1995). Beyond the turbidite paradigm: physical models for deposition of turbidites and their implications for reservoir prediction. In: *Characterization of deep marine clastic systems*. A.J. Hartley (Ed). Pp. 31-49, Geological Society London. ISBN: 1897799357. London, UK.
- Kneller, B.C., Bennett, S.J. & McCaffrey, W.D. (1999) Velocity structure, turbulence and fluid stresses in experimental gravity currents. *Journal of Geophys. Research. Oceans.*, Vol. 94, pp. 5281-5291.
- Kneller, B. & Buckee, C. (2000). The structure and fluid mechanics of turbidity currents: a review of some recent studies and their geological implications. *Sedimentology*, Vol.47, Suppl. 1, pp. 62-94, ISSN 0091-7613.



- Kuenen, P. H. (1950). Turbidity currents of high density. In: *Proceedings of 18<sup>th</sup> International Geological Congress (1948)*, London, pp. 44-52.
- Lowe, D. R. (1979). Sediment gravity flows: Their classification and some problems of application to natural flows and deposits. *SEPM (Special Publication n. 27)*, pp 75-82.
- Lowe, D. R. (1982). Sediment gravity flows: II. Depositional models with special reference to the deposits of high-density turbidity currents. *Journal of Sedimentary Petrology*, Vol. 52, No. 1, pp. 279-297.
- Normark, W.R. & Piper, D. J. W. (1991). Initiation processes and flow evolution of turbidity currents: implications for the depositional record. *SEPM (Special Publication n. 46)*. pp. 207-230.
- Manica, R. (2009). *Correntes de turbidez de alta densidade: condicionantes hidráulicos e deposicionais*. PhD thesys, Instituto de Pesquisas Hidráulicas, Universidade Federal do Rio Grande do Sul, Porto Alegre - Brazil.
- Marr, J.G., Harff, P.A., Shanmugan, G. & Parker, G. (2001) Experiments on subaqueous sandy gravity flow: the role of clay and water content in flow dynamics and depositional structures. *GSA Bulletin*, Vol. 113, No. 11, pp. 1377-1386.
- McCave, I. N & Jones, P.N (1988). Deposition of ungraded muds from high-density non turbulent turbidity currents. *Nature*, Vol. 333, pp 250-252, ISSN 0016-7649
- Michon, X.; Goddet, J. & Bonnefille, R. (1955). *Etude Theorique et experimentale des courants de densite*. 2 vol. Lab. Nat. d'Hydraulique Chatou, França.
- Middleton, G. V. (1966). Experiments on density and turbidity currents I. Motion of the head. *Canadian Journal of Earth Sciences*, Ottawa, Vol. 3, pp. 523-546.
- Middleton, G. V. (1993). Sediment deposition from turbidity currents. *Annual Review of Earth Planet Science*, Vol. 21, pp. 89-114.
- Middleton, G. V. & Hampton, M. A. (1973). Sediment gravity flows: mechanics of flow and deposition. In *Turbidites and Deep Water Sedimentation* G. V. Middleton and A. H. Bouma (eds.). Anaheim, California, SEPM. Short Course Notes, 38p
- Mohrig, D.; Elverhoi, A.; & Parker, G. (1999). Experiments on the relative mobility of muddy subaqueous and subaerial debris flows, and their capacity to remobilize antecedent deposits. *Marine Geology*. Vol. 154, pp. 117-129.
- Mohrig, D. & Marr, J.G. (2003). Constraining the efficiency of turbidity current from submarine debris flow and slides using laboratory experiments. *Marine and Petroleum Geology*, Vol. 20, pp. 883-899
- Parker, G., Fukushima, Y., & Pantin, H.M., (1986). Self accelerating turbidity currents: *Journal of Fluid Mechanics*, Vol. 171, pp. 145-181.
- Parker, G., Garcia, M., Fukushima, Y. & YU, W. (1987) Experiments on turbidity currents over a erodible bed. *Journal of Hydraulic Research*, Vol. 25, pp. 123-147.
- Parsons, J. D; Friedrichs C. T.; Traykovsky P. A.; Mohrig, D.; Imran, J.; Syvitsky, P. M.; Parker, G.; Puig, P.; Buttle, J. L. & Garcia, M. H. (2010). The mechanics of sediment gravity flows. In *Continental Margin Sedimentation: From Sediment Transport to Sequence Stratigraphy*. C. A. Nittrouer, J. A. Austin, M. E. Field, J. H. Kravitz, J. P. M. Syvitski, P. L. Wiberg, John Wiley & Sons, ISBN 9781405169349, New York, US.
- Postma, G.; Nemec, W. & Kleinspehn, K.L. (1988). Large floating clasts in turbidites: a mechanism for their emplacement. *Sedimentary Geology*, Vol. 58, pp. 47-61.
- Simpson, E. J. (1972). Effects of the lower boundary on the head of a gravity current. *Journal of Fluid Mechanics*, Vol. 53, pp. 759-768.

- Simpson, E. J. (1997). *Gravity currents in the environment and the laboratory*. 2.ed. Cambridge University, ISBN 0521664012, UK
- Talling, P. J.; Wynn, R. B.; Masson, D. G., Frenz, M.; Cronin, B. T.; Schiebel, R.; Akhmetzhanov, A. M., Dallmeier-Tiessen, S., Benetti, S.; Weaver, P. P. E.; Georgiopoulou, A.; Zuhlsdorff, C. & Amy, L. A. (2007). Onset of submarine debris flow deposition far from original giant landslide. *Nature*. Vol. 450. pp. 541-544
- Wan, Z.; & Wang, Z., (1994),. *Hyperconcentrated Flow*. IAHR Monograph Series, A. A. Balkema. Rotterdam. 290p
- Whitehouse, R., Soulsby, R., Roberts, W. & Mitchener, H. (2000). *Dynamics of Estuarine Muds*. London, UK.
- Winterwerp, J. C. (2001). Stratification effects by cohesive and non-cohesive sediment, *J. Geophys. Research*, Vol. 106, No. 22, pp. 559 -574.
- Winterwerp, J.C. (2002). On the flocculation and settling velocity of estuarine mud. *Cont. Shelf Research*. Vol. 22, pp. 1339–1360.

IntechOpen



## **Hydrodynamics - Natural Water Bodies**

Edited by Prof. Harry Schulz

ISBN 978-953-307-893-9

Hard cover, 286 pages

**Publisher** InTech

**Published online** 05, January, 2012

**Published in print edition** January, 2012

The knowledge of the characteristics of the fluids and their ability to transport substances and physical properties is relevant for us. However, the quantification of the movements of fluids is a complex task, and when considering natural flows, occurring in large scales (rivers, lakes, oceans), this complexity is evidenced. This book presents conclusions about different aspects of flows in natural water bodies, such as the evolution of plumes, the transport of sediments, air-water mixtures, among others. It contains thirteen chapters, organized in four sections: Tidal and Wave Dynamics: Rivers, Lakes and Reservoirs, Tidal and Wave Dynamics: Seas and Oceans, Tidal and Wave Dynamics: Estuaries and Bays, and Multiphase Phenomena: Air-Water Flows and Sediments. The chapters present conceptual arguments, experimental and numerical results, showing practical applications of the methods and tools of Hydrodynamics.

### **How to reference**

In order to correctly reference this scholarly work, feel free to copy and paste the following:

Rafael Manica (2012). Sediment Gravity Flows: Study Based on Experimental Simulations, Hydrodynamics - Natural Water Bodies, Prof. Harry Schulz (Ed.), ISBN: 978-953-307-893-9, InTech, Available from: <http://www.intechopen.com/books/hydrodynamics-natural-water-bodies/sediment-gravity-flows-study-based-on-experimental-simulations>

**INTECH**  
open science | open minds

### **InTech Europe**

University Campus STeP Ri  
Slavka Krautzeka 83/A  
51000 Rijeka, Croatia  
Phone: +385 (51) 770 447  
Fax: +385 (51) 686 166  
[www.intechopen.com](http://www.intechopen.com)

### **InTech China**

Unit 405, Office Block, Hotel Equatorial Shanghai  
No.65, Yan An Road (West), Shanghai, 200040, China  
中国上海市延安西路65号上海国际贵都大饭店办公楼405单元  
Phone: +86-21-62489820  
Fax: +86-21-62489821

© 2012 The Author(s). Licensee IntechOpen. This is an open access article distributed under the terms of the [Creative Commons Attribution 3.0 License](https://creativecommons.org/licenses/by/3.0/), which permits unrestricted use, distribution, and reproduction in any medium, provided the original work is properly cited.

IntechOpen

IntechOpen